

Exploring the Potential of VGG-16 Architecture for Accurate Brain Tumor Detection Using Deep Learning

Prerepa Gayathri^{1,2}, Aiswarya Dhavileswarapu³, Sufyan Ibrahim⁴, Rahul Paul*⁵, and Reena Gupta⁶

¹Department of Electrical and Computer Engineering, NYU Tandon School of Engineering, NYU Tandon School of Engineering, New York University, New York, United States 11201

²Department of Electronics and Communication, Manipal Institute of Technology, Manipal Academy of Higher Education, Manipal, Karnataka, India 576104

³Department of Electronics and Communication, GITAM University, Gandhi Nagar, Rushi Konda, Visakhapatnam, Andhra Pradesh, India 530045

⁴Neuro-Informatics Laboratory, Department of Neurological Surgery, Mayo Clinic, Rochester, Minnesota, USA 55905

⁵Department of Radiation Oncology, Massachusetts General Hospital, Harvard Medical School, Boston, Massachusetts, USA 02115

⁶Department of Pharmacognosy, Institute of Pharmaceutical Research, GLA University, Mathura 281406, Uttar Pradesh, India 281406

Abstract

This study explores the potential of the VGG-16 architecture, a Convolutional Neural Network (CNN) model, for accurate brain tumor detection through deep learning. Utilizing a dataset consisting of 1655 brain MRI images with tumors and 1598 images without tumors, the VGG-16 model was fine-tuned and trained on this data. Initial training achieved an accuracy of 91%, which was improved to 94% after hyperparameter optimization. The model's sensitivity, specificity, precision, recall, and F1 scores were strong, indicating its potential in accurately detecting brain tumors. The performance of the VGG-16 model was compared to several other techniques for brain tumor detection, including EasyDL, GoogLeNet, GrayNet, ImageNet, CNN, and a Multivariable Regression and Neural Network model. Although it did not achieve the highest accuracy, it outperformed GoogLeNet and ImageNet and demonstrated comparable accuracy to GrayNet and the Multivariable Regression and Neural Network. Its sensitivity and specificity suggest its potential in identifying tumors that other methods might miss, reinforcing its potential usefulness in medical applications. Nevertheless, there is room for improvement. Future studies could collect and annotate larger datasets to improve model generalizability. Exploring other deep learning architectures and enhancing model interpretability could further boost its clinical relevance. Despite these challenges, this study demonstrates the untapped potential of the VGG-16 architecture in brain tumor detection and contributes to the growing body of research on applying deep learning in the medical field.

Keywords: VGG-16 Architecture; Brain Tumor Detection; Deep Learning; Convolutional Neural Network (CNN); Accuracy

1 Introduction

Brain tumors, characterized by abnormal cell proliferation within the brain, pose a critical health challenge [1, 2]. As the brain is confined within the rigid skull, any undue expansion can lead to severe complications, making early and accurate detection vital for effective treatment [3–5].

*Corresponding author: rahul.paul@usf.com

Received: 06 April 2023; **Accepted:** 31 May 2023; **Published:** 06 June 2023

© 2023 Journal of Computers, Mechanical and Management.

This is an open access article and is licensed under a [Creative Commons Attribution-Non Commercial 4.0 International License](https://creativecommons.org/licenses/by-nc/4.0/).

DOI: [10.57159/gadl.jcmm.2.2.23056](https://doi.org/10.57159/gadl.jcmm.2.2.23056).

Traditionally, detection involved an expert examination of medical images, primarily magnetic resonance imaging (MRI) scans. However, this approach can be time-consuming and potentially lead to missed or incorrect diagnoses [6–8]. Deep Learning (DL), a subfield of machine learning, has emerged as a powerful tool showing significant promise in various domains, notably in image recognition and analysis. DL systems have the potential to reduce human effort significantly and have revolutionized many sectors, including healthcare. However, applying DL to MRI-based brain tumor detection presents challenges and limitations. These include issues related to image quality, high degrees of anatomical variations, and the need for domain-specific expert interpretation [9–13]. Overcoming these challenges is a significant factor that can dramatically influence the effectiveness and reliability of DL models and understanding these challenges is integral to the context of the current study. Figure 1 outlines the general architecture of a deep neural network.

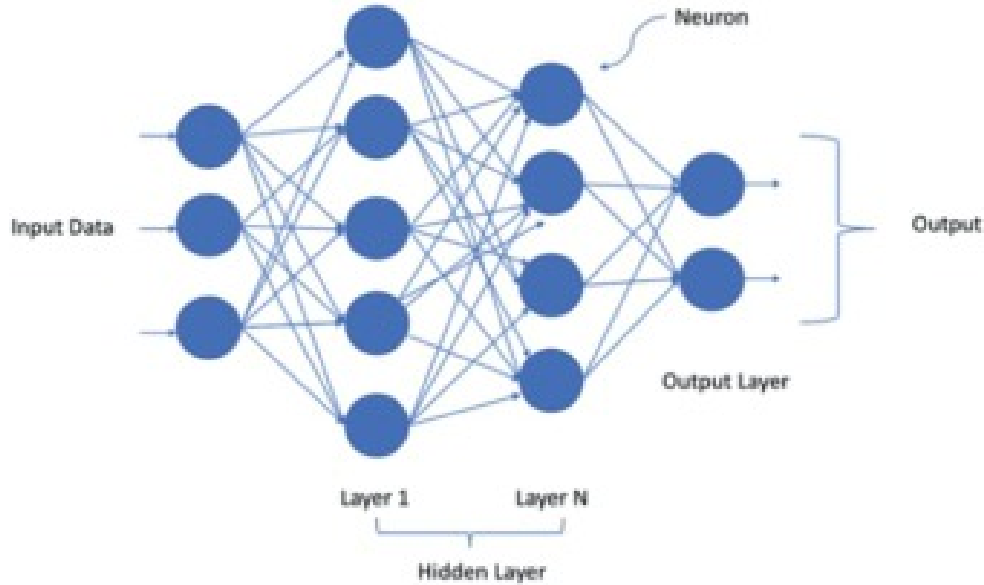


Figure 1: Deep neural network architecture [14].

While the potential advantages of the VGG-16 architecture in brain tumor detection are briefly mentioned in few of the earlier studies [15, 16], a more detailed context about the state-of-the-art models in this field is required. A comprehensive comparison of the VGG-16 architecture with these models will provide readers with a clearer perspective on our study’s novelty and unique contributions. It would also explain why VGG-16 warrants exploration for brain tumor detection, considering its successful application in other image analysis tasks. In other words, the present study explores the untapped potential of the VGG-16 architecture, a Convolutional Neural Network (CNN) model, for accurate brain tumor detection through deep learning. By developing a model for diagnosing and detecting brain tumors using MRI images, the work aims to significantly reduce diagnosis time compared to conventional methods while ensuring high accuracy and efficiency.

2 Related Work

Deep learning techniques have been extensively employed in cancer/tumor detection, with numerous studies aiming to enhance their accuracy and efficiency. Each study, however, has unique aspects related to the type of cancer or tumor investigated, the deep learning techniques employed, the performance metrics used, and the datasets utilized. These variables might influence the generalizability of the models to other datasets. By grouping the studies based on specific cancer or tumor types and the deep learning technique used, we can discern commonalities and differences and understand their implications for our current study. Numerous studies have leveraged convolutional neural networks (CNN) for cancer/tumor detection and segmentation. For instance, Yang et al. [17] used EasyDL and GoogLeNet, achieving impressive detection efficiencies of 96.9% and 92.54% respectively. Similarly, Cha et al. [18] developed a deep learning CNN (DLCNN) to distinguish the interior and exterior of the bladder. However, these studies are limited by the size and type of datasets used, which might restrict the applicability of the models to more diverse datasets. Some studies employed other deep learning techniques. Lorencin et al. [19] used a Multi-Layer Perceptron (MLP) with a Laplacian edge detector, while Harmon et al. [20] employed a multivariable logistic regression and neural network model for prediction, achieving an accuracy of 95%. Despite these promising results, the potential generalizability of these models to other datasets requires further investigation. In terms of segmentation, Ma et al. [21] utilized deep learning frameworks, specifically, fully convolutional residual networks (FCRN) and U-Net based deep learning techniques (U-DL), respectively. They improved the segmentation of cancerous regions in medical images, illustrating the potential of deep learning for precise tumor localization. Deep learning techniques have also been used for classifying various types of cancer. Coudray et al. [22] used CNN to categorize whole-slide images of lung tissue with remarkable results. Similarly, Cruz-Roa et al. [23] and Bar et al. [24] employed deep learning algorithms for pathology identification, showcasing their potential in this domain. However, limitations in these studies, such as the size and specificity of the datasets used, may affect the generalizability of their models.

While previous studies demonstrate the potential of deep learning techniques in cancer/tumor detection, limitations regarding dataset size and diversity, and the specificity of the models developed, suggest a need for additional research. Understanding these limitations can help inform and refine the development of our VGG-16 architecture-based model for brain tumor detection using MRI images.

3 VGG-16 Architecture

3.1 Description of VGG-16 architecture

The VGG-16 architecture, also known as the Visual Geometry Group-16, is a deep learning model created by researchers at the University of Oxford [25]. This Convolutional Neural Network (CNN) is specifically designed for image recognition and classification tasks [26–28]. VGG-16 is renowned for its simplicity and relatively lower computational complexity compared to other deep learning architectures like ResNet and Inception [29]. The architecture consists of a total of 16 weight layers, including 13 convolutional layers, 3 fully connected layers, and 5 max-pooling layers [30].

3.2 The 16-layer structure

The VGG-16's 16-layer structure is organized hierarchically, with each layer building upon the features extracted from the preceding layer [31]. The input layer, which receives the input image data. This data is typically resized to a fixed dimension (e.g., 224×224 pixels) before being introduced to the network [32]. There are 13 convolutional layers, each responsible for extracting features from the input image using a series of filters or kernels. Each filter slides over the input data, performing element-wise multiplication and summation to generate a feature map. Notably, the convolutional layers in VGG-16 employ small 3×3 filters, enabling the network to learn more complex patterns with fewer parameters. Following each convolutional layer, an activation layer applies a Rectified Linear Unit (ReLU) activation function. This step introduces non-linearity into the model, allowing it to learn more intricate patterns. The architecture includes five pooling layers, which reduce the spatial dimensions of the feature maps, helping decrease computational complexity and control overfitting. VGG-16 uses max-pooling, which retains the maximum value within each pooling window. Lastly, there are three fully connected layers, which combine the features extracted from the previous layers and make the final predictions. The last of these fully connected layers utilizes a softmax activation function to output probabilities for each class [30, 33–36].

3.3 Convolution and pooling layers

The convolution and pooling layers are the foundational components of the VGG-16 architecture. They enable the network to learn hierarchical feature representations from the input image data [37, 38]. The convolution layers perform a pivotal role in the VGG-16 architecture by extracting features from the input images using a series of filters or kernels. These filters are small matrices with specific dimensions (e.g., 3×3), which slide across the input data, executing element-wise multiplication and summation with the underlying input data. The result is a feature map that provides a higher-level abstraction of the input image. Throughout the VGG-16 architecture, the convolution layers utilize small 3×3 filters. These filters allow the model to learn more complex patterns and hierarchical representations with fewer parameters than larger filter sizes would require. As the network progresses through multiple convolution layers, the filters learn to capture increasingly complex and abstract features. This hierarchical feature extraction process enables the model to discern intricate patterns within the images, contributing to its effectiveness in image recognition and classification tasks. The pooling layers have an essential role in reducing the spatial dimensions of the feature maps produced by the convolution layers. By down sampling the feature maps, the pooling layers decrease computational complexity and aid in controlling overfitting, thereby ensuring that the model generalizes well to unseen data. In the VGG-16 architecture, max-pooling is used in the pooling layers. Max-pooling operates by selecting the maximum value within each pooling window (e.g., 2×2) and discarding the remaining values. This operation effectively retains the most prominent features while reducing the size of the feature maps. Max-pooling is applied after specific convolution layers, resulting in a total of five pooling layers throughout the network [30, 33–36].

3.4 Advantages of Using VGG-16 architecture

The VGG-16 architecture offers numerous advantages when applied to image recognition and classification tasks. The simplicity of the VGG-16 architecture, facilitated by the use of small 3×3 filters and an uncomplicated architecture, makes it easy to understand and implement. Compared to other deep learning architectures, VGG-16 requires fewer parameters, which reduces the computational resources needed for training and inference, hence offering lower computational complexity. The pre-trained VGG-16 model can be fine-tuned for various tasks, allowing researchers to leverage the knowledge obtained from large-scale datasets like ImageNet and adapt it to specific applications with relatively smaller datasets. This is known as transfer learning. Finally, the hierarchical structure of the VGG-16 architecture allows the model to learn robust and discriminative feature representations, making it suitable for various image recognition and classification tasks, including medical image analysis [29, 30, 39].

4 Methodology

A comprehensive methodology is crucial for the successful implementation of the VGG-16 architecture for accurate brain tumor detection. The following sections detail the various steps involved in the process.

4.1 Dataset

The dataset used in this study consisted of Magnetic Resonance Imaging (MRI) scans of the brain, comprising 1655 images with tumors and 1598 images without tumors. It was diverse and represented various tumor types, sizes, and stages. The data was sourced from two publicly available online repositories, namely the Brain Tumor Dataset from the Cancer Imaging Archive (TCIA) and the Brain MRI Images for Brain Tumor Detection from Kaggle. The Cancer Imaging Archive (TCIA) is an open-access database that provides a large collection of medical images for research purposes. The specific dataset used from TCIA can be accessed at www.cancerimagingarchive.net. In addition, the Brain MRI Images for Brain Tumor Detection dataset from Kaggle, an open-source platform for predictive modelling and analytics competitions, was also used. The dataset can be accessed at www.kaggle.com. These databases offer curated datasets for research purposes, contributing to the robustness and diversity of our dataset.

Once obtained, the dataset was split into three subsets for training, validation, and testing, maintaining a ratio of 80:10:10, respectively. This separation ensured that the model could be trained and fine-tuned on a significant portion of the data, while also being evaluated fairly and independently on unseen data for validation and testing.

4.2 Implementation of VGG-16 architecture for brain tumor detection

4.2.1 Preprocessing

Preprocessing of MRI images is pivotal to ensure the effective learning capability of the VGG-16 model from the input data. The initial step in preprocessing medical image data involves cropping the extra regions from the MRI scans. To accomplish this, images were first blurred to soften well-defined boundaries. Subsequently, contours were identified using an inbuilt function such as `cv2.findContours`. Given that pixels are stored in array form, the extreme points of the region of interest were found using `max` and `min` functions. Any pixels falling outside this boundary were then eliminated. The subsequent step entails visualizing the data to evaluate the quality of the images and determine any further modifications required. A function was developed to display images from a specific folder, enabling the user to view random samples from the dataset. For instance, by invoking this function with the training set as a parameter and specifying the number of images 'n' as 30, the function would display 30 random images from the 'yes' and 'no' folders within the training dataset. Images were displayed in a grid format, also known as subplots. In this instance, a 10x3 subplot was created, but other configurations, such as 5x6, can also be employed. To acquire an approximate understanding of the dimensions of the cropped images, a histogram was generated. This visualization aided in determining whether or not the images required resizing. In most instances, images were not uniform in size and hence required resizing for computational purposes. Based on the histogram analysis, it was determined that the images required resizing. As a result, MRI scans were resized to dimensions of 224 x 224 pixels, compatible with the input requirements of the VGG-16 model. The resized images were then normalized to ensure a consistent range of pixel values. Finally, data augmentation techniques were employed to enhance the diversity of the training dataset and improve the model's generalization capabilities.

4.2.2 Transfer Learning

The VGG-16 model pretrained on a large-scale dataset, such as ImageNet, can be fine-tuned to adapt to the specific task of brain tumor detection. The final fully connected layer of the pretrained model should be replaced with a new layer that outputs the appropriate number of classes (e.g., tumor or no tumor). The model can then be trained on the labeled MRI scans using backpropagation and optimization algorithms, such as stochastic gradient descent or Adam. In this case, the model was trained on approximately 2500 images. Initially, the model was trained with 10 epochs and a batch size of 150, which took 17 cycles per epoch and 2 hours to train, achieving an accuracy of 91% on the training set. After tweaking the values, the number of epochs was increased to 11, and the batch size was adjusted to 250. This configuration took 10 cycles per epoch and 2 hours to train, resulting in an improved accuracy of 94% on the training set. A graph of the model's loss and accuracy versus the number of epochs was plotted, showing that the loss decreased and accuracy increased as the number of epochs increased, indicating that the model had learned effectively.

4.2.3 Fine tuning

The learning rate, batch size, and other hyperparameters should be tuned to optimize the model's performance. Regularization techniques, such as dropout or weight decay, can be employed to prevent overfitting. In this project, the batch size was fine-tuned to achieve better performance. When tested, the final model achieved an accuracy of 93

5 Evaluation of Model Performance

To evaluate the performance of a model, several metrics can be used. These metrics help to assess the model's effectiveness in predicting the correct outcomes and handling false positives and false negatives. A confusion matrix is a common tool for visualizing the performance of a model, as shown in Table 1.

Table 1: Confusion matrix

	Predicted Negative	Predicted Positive
Actual Negative	True Negative	False Positive
Actual Positive	False Negative	True Positive

The confusion matrix consists of four components:

- **True Positives (TP):** These represent the cases where both the actual and predicted class values are positive. For example, if the actual class value indicates that a passenger survived and the predicted class also indicates that the passenger survived.
- **True Negatives (TN):** These represent the cases where both the actual and predicted class values are negative. For example, if the actual class value indicates that a passenger did not survive, and the predicted class also indicates that the passenger did not survive.
- **False Positives (FP):** These occur when the actual class value is negative, and the predicted class value is positive. For example, if the actual class value indicates that a passenger did not survive, but the predicted class value indicates that the passenger survived.
- **False Negatives (FN):** These occur when the actual class value is positive, and the predicted class value is negative. For example, if the actual class value indicates that a passenger survived, but the predicted class value indicates that the passenger did not survive.

Several performance metrics can be derived from the confusion matrix:

- **Accuracy:** The ratio of correctly predicted observations to all observations. It is a useful metric when the datasets have symmetric false positives and false negatives. The same is mathematically represented by Eq.1.

$$Accuracy = (TP + TN) / (TP + FP + FN + TN) \quad (1)$$

- **Precision:** The ratio of correctly predicted positive observations to total predicted positive observations. It is related to the false positive rate and mathematically represented by Eq.2.

$$Precision = TP / (TP + FP) \quad (2)$$

- **Recall (Sensitivity):** The ratio of correctly predicted positive observations to the total observations in the actual class, which is mathematically represented by Eq.3.

$$Recall = TP / (TP + FN) \quad (3)$$

- **F1 Score** - The weighted average of Precision and Recall. It is more useful than accuracy when the class distribution is unequal, or when false positives and false negatives have different costs and is mathematically represented by Eq.4.

$$F1Score = 2(Recall \times Precision) / (Recall + Precision) \quad (4)$$

By analyzing these metrics, a better understanding of the model's performance and identify areas for improvement were gained in the present work.

6 Results and Discussion

6.1 Presentation of intermediate results

Figure 2 represents the obtained confusion matrix. The matrix was used to evaluate the VGG-16 model's performance in brain tumor detection using various metrics (discussed in the earlier sections) to assess its effectiveness. The intermediate results obtained for

each metric is represented in Table 2. The performance of the VGG-16 model for brain tumor detection was thoroughly evaluated using a comprehensive set of metrics derived from a confusion matrix, including sensitivity, specificity, precision, recall, and the F1 score. The model exhibited a high sensitivity of 93.97%, indicating its robust ability to correctly identify cases with brain tumors. This implies that our model successfully detected approximately 94% of the positive cases from the total actual positive cases. This high level of sensitivity is particularly crucial in medical diagnostics, where failing to detect a condition, such as a tumor, could lead to severe consequences.

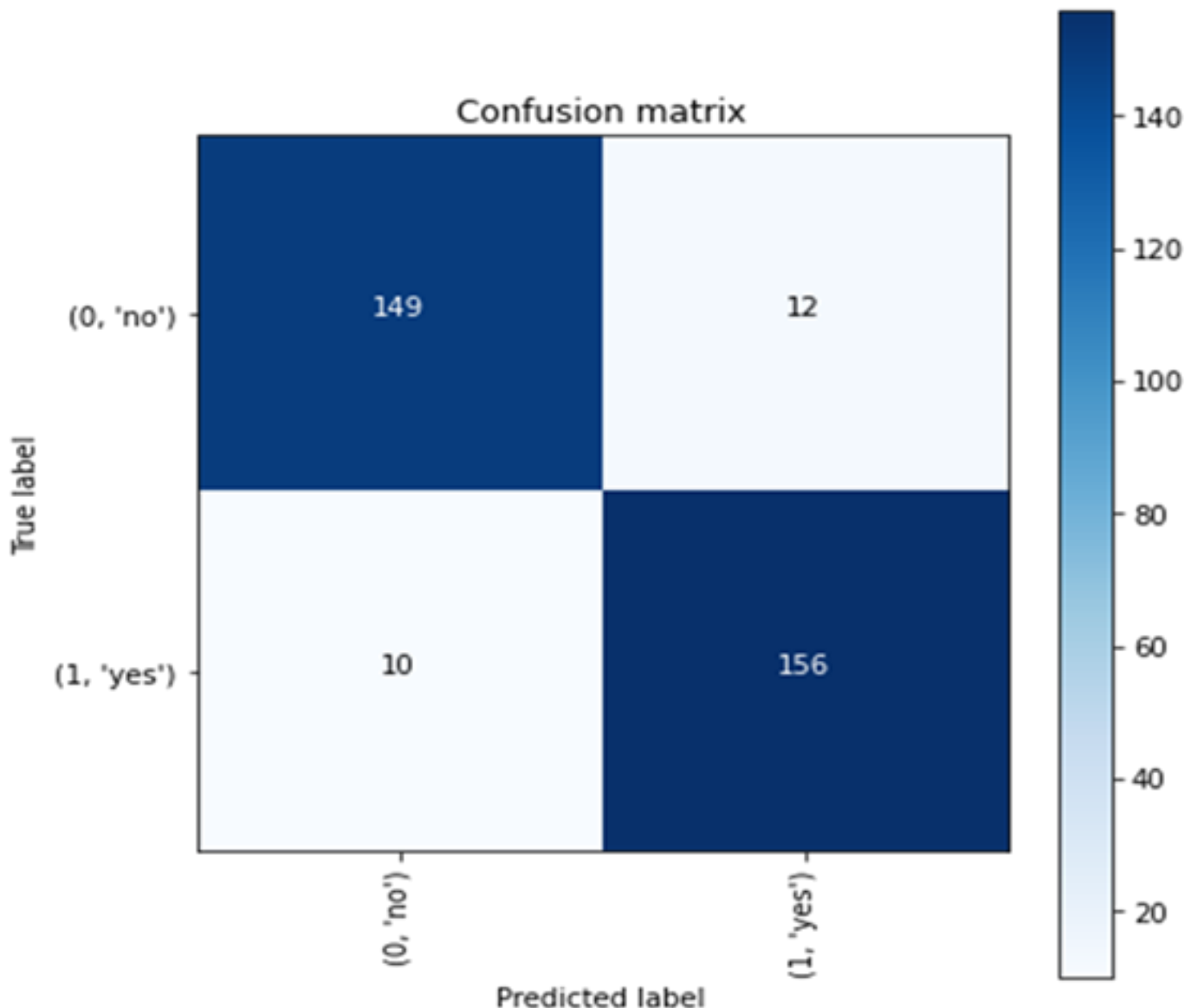


Figure 2: Confusion matrix obtained for the dataset

Furthermore, the model’s specificity was recorded at 92.54%, reflecting its proficiency in accurately identifying negative cases, i.e., scans without tumors. This suggests that the model correctly classified about 93% of the actual negative cases, thus demonstrating its effectiveness in avoiding false positives. The precision score was another important metric used to evaluate the performance of our model. The precision score was found to be 93.28%, indicating that when our model predicted a positive case (presence of a tumor), it was correct approximately 93% of the time. This level of precision can greatly assist clinicians by providing reliable predictions, thus reducing the risk of false-positive diagnosis. The recall score, which is identical to sensitivity in binary classification problems, was found to be 93.27%, reiterating the model’s strong ability to identify all actual positive cases accurately. Lastly, the F1 score, which represents the harmonic mean of precision and recall, was computed to be 93.27%. A high F1 score signifies a well-balanced model in terms of recall and precision, indicating that our model is neither excessively biased towards false positives nor false negatives. This balance is vital in ensuring a robust and reliable diagnostic model. From the obtained results, it could be inferred that the strong performance metrics demonstrated by our VGG-16 model suggest its significant potential for effective and reliable brain tumor detection from MRI scans. This success opens up avenues for further research into the application of deep learning architectures for medical diagnostic tasks. Future work could involve refining the model and validating its effectiveness on a larger, more diverse dataset, thus paving the way for a reliable, AI-assisted diagnostic tool in neurology.

Table 2: Model performance metrics

Metric	Value
Sensitivity	0.9397
Specificity	0.9254
Precision score	0.9328
Recall score	0.9327
F1 Score	0.9327

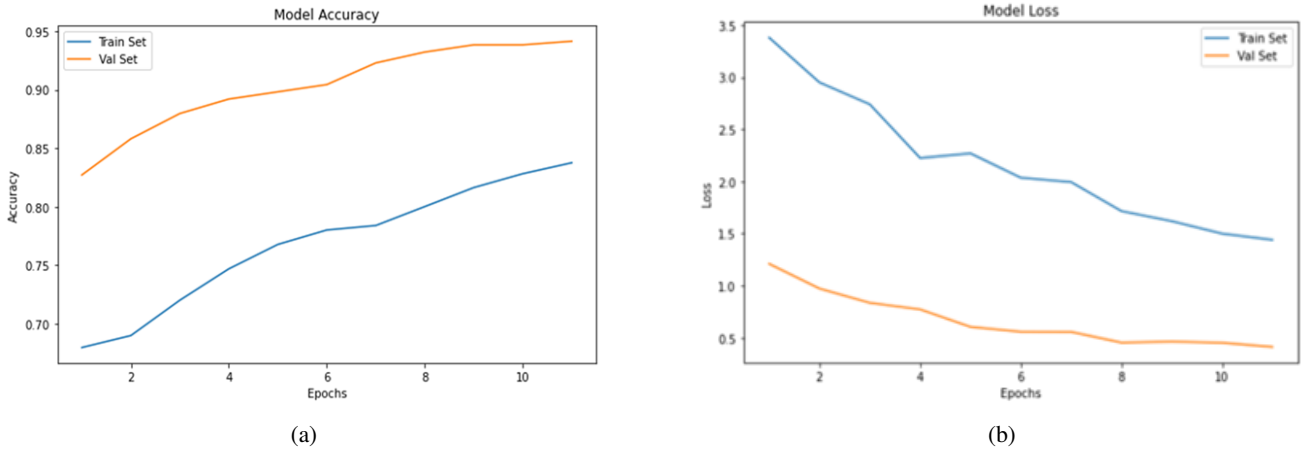


Figure 3: Relationship between model performance (a) accuracy versus number of epochs; (b) model loss versus number of epochs.

Figure 3 delineate the relationship between model performance and the number of training epochs, offering essential insights into the learning dynamics of the machine learning model throughout the training phase. Figure 3 demonstrates that both the training and validation accuracy show a predominantly increasing trend with a growing number of epochs, a promising indication of the model’s learning capability and its proficiency in generalizing unseen data. While there exist sporadic minor dips in the accuracy, they are negligible in the grand scheme of the training process due to the overarching upward trajectory. This progressive increase in accuracy suggests that the model strikes a healthy balance between learning and generalizing - it neither overfits to the training data nor underfits by failing to capture the necessary patterns. Nonetheless, continued observation is warranted until the accuracy for both training and validation sets attains a plateau or reaches a satisfactory threshold, which signifies the model’s convergence. Figure 4 presents a mirror image of the preceding scenario - the model loss for both training and validation sets exhibits a steady decrease as the number of epochs progresses. This downward trajectory in loss underpins the efficacy of the model’s learning strategy, signifying the minimization of discrepancies between the model’s predictions and the actual targets. The dwindling model loss attests to the fact that, as the training unfolds across epochs, the model hones its prediction-making skills, leading to more precise outputs. In a nutshell, the overall performance of the model appears to be promising, shedding light on the potential of deep learning architectures in the domain of medical image analysis.

6.2 Comparison of VGG-16 model performance to existing techniques

To furnish a comprehensive understanding of the VGG-16 model’s competitive standing in the realm of brain tumor detection, its accuracy was juxtaposed with several other established models. Table 3 elucidates this comparison with the respective accuracies of the models.

Table 3: Comparison of Model Accuracies

Model	Accuracy
VGG-16 (my model)	93%
EasyDL	96.6%
GoogLeNet	92.54%
GrayNet	95%
ImageNet	91%
CNN	96%
Multivariable Regression and Neural Network	95%

Albeit not claiming the accolade of the most accurate model, the VGG-16 model's performance puts forth a strong competition. The model boasts superior accuracy than GoogLeNet and ImageNet, while demonstrating a performance on par with the likes of GrayNet and the Multivariable Regression and Neural Network model. This comparative examination underlines the considerable potential that the VGG-16 model embodies for the task of brain tumor detection. However, the pursuit of further enhancements remains imperative to either match or exceed the prowess of the top-tier models in the field.

7 Conclusion

The rising prominence of Convolutional Neural Networks (CNNs) has revolutionized image classification and segmentation across various fields. While designing a custom CNN is intricate due to decisions regarding layers, filter sizes, padding types, and more, pre-trained models like VGG-16 offer a powerful alternative. Despite its extensive use in other domains, its applicability in brain tumor detection remained unexplored, prompting this investigation. The VGG-16 model used in the present work demonstrated promising results, achieving a 93% accuracy rate in detecting brain tumors. Performance metrics including sensitivity, specificity, precision, recall, and F1 score further validated the model's efficacy. Compared to established techniques, the VGG-16 model showcased competitive performance—exceeding GoogLeNet, GrayNet, and ImageNet, albeit falling short of EasyDL and CNN. This underscores the potential of the VGG-16 architecture in brain tumor detection, necessitating further exploration. Looking ahead, the integration of CNNs in medical imaging signifies a significant stride in healthcare. As the field matures, more refined CNN models may facilitate superior diagnosis accuracy for brain tumors and other medical conditions. Delving into alternate imaging modalities, such as MRI and PET, might augment the detection precision further. There is also an exciting prospect in developing automated diagnostic and treatment systems using CNN models, which could profoundly transform the healthcare industry. In conclusion, this study substantiates the pivotal role of CNNs and pre-trained models like VGG-16 in medical image analysis. As research advances and these models are further refined, they hold the potential to revolutionize diagnosis and treatment accuracy in healthcare.

Declaration of Competing Interests

The authors declare that they have no known competing financial interests or personal relationships that could have appeared to influence the work reported in this paper.

Funding Declaration

This research did not receive any grants from governmental, private, or nonprofit funding bodies.

Author Contribution

Prerepa Gayathri: Conceptualization, Data curation, Formal analysis, Investigation, Methodology, Validation; **Aiswarya Dhavileswarapu:** Data curation, Formal analysis, Investigation, Methodology, Software; **Sufyan Ibrahim:** Data curation, Formal analysis, Investigation, Methodology, writing: review and editing; **Rahul Paul:** Conceptualization, Methodology, Project administration, Supervision, Roles/writing: original draft, writing: review and editing; **Reena Gupta:** Conceptualization, Investigation, Resources, Supervision, writing: review and editing.

References

- [1] G. S. Tandel, M. Biswas, O. G. Kakde, A. Tiwari, H. S. Suri, M. Turk, J. Laird, C. Asare, A. A. Ankrah, N. N. Khanna, B. K. Madhusudhan, L. Saba, and J. S. Suri, "A Review on a Deep Learning Perspective in Brain Cancer Classification," *Cancers*, vol. 11, p. 111, jan 2019.
- [2] Sheila K Singh, Ian D Clarke, Mizuhiko Terasaki, Victoria E Bonn, Cynthia Hawkins, Jeremy Squire, and Peter B Dirks, "Identification of a Cancer Stem Cell in Human Brain Tumors," *Cancer Research*, vol. 63, pp. 5821–5828, 2003.
- [3] E. U. Haq, J. Huang, L. Kang, H. U. Haq, and T. Zhan, "Image-based state-of-the-art techniques for the identification and classification of brain diseases: a review," *Medical & Biological Engineering & Computing*, vol. 58, pp. 2603–2620, nov 2020.
- [4] F. G. Kengne and G. Decaux, "CNS Manifestations of hyponatremia and its treatment," *Hyponatremia: Evaluation and Treatment*, pp. 87–110, 2013.

- [5] R. J. Forsyth, J. Raper, and E. Todhunter, "Routine intracranial pressure monitoring in acute coma," *Cochrane Database of Systematic Reviews*, vol. 2016, nov 2015.
- [6] A. Tiwari, S. Srivastava, and M. Pant, "Brain tumor segmentation and classification from magnetic resonance images: Review of selected methods from 2014 to 2019," *Pattern Recognition Letters*, vol. 131, pp. 244–260, mar 2020.
- [7] A. K. Sharma, A. Nandal, A. Dhaka, and R. Dixit, "A survey on machine learning based brain retrieval algorithms in medical image analysis," *Health and Technology*, vol. 10, pp. 1359–1373, nov 2020.
- [8] G. Mohan and M. M. Subashini, "MRI based medical image analysis: Survey on brain tumor grade classification," *Biomedical Signal Processing and Control*, vol. 39, pp. 139–161, jan 2018.
- [9] M. W. Nadeem, M. A. Al Ghamdi, M. Hussain, M. A. Khan, K. M. Khan, S. H. Almotiri, and S. A. Butt, "Brain tumor analysis empowered with deep learning: A review, taxonomy, and future challenges," *Brain Sciences*, vol. 10, no. 2, 2020.
- [10] X. Zhao and X. M. Zhao, "Deep learning of brain magnetic resonance images: A brief review," *Methods*, vol. 192, pp. 131–140, 2021.
- [11] J. Bernal, K. Kushibar, D. S. Asfaw, S. Valverde, A. Oliver, R. Martí, and X. Lladó, "Deep convolutional neural networks for brain image analysis on magnetic resonance imaging: a review," *Artificial Intelligence in Medicine*, vol. 95, pp. 64–81, 2019.
- [12] S. Somasundaram and R. Gobinath, "Current Trends on Deep Learning Models for Brain Tumor Segmentation and Detection - A Review," *Proceedings of the International Conference on Machine Learning, Big Data, Cloud and Parallel Computing: Trends, Perspectives and Prospects, COMITCon 2019*, pp. 217–221, 2019.
- [13] M. Tanveer, M. A. Ganaie, I. Beheshti, T. Goel, N. Ahmad, K.-T. Lai, K. Huang, Y.-D. Zhang, J. Del Ser, and C.-T. Lin, "Deep Learning for Brain Age Estimation: A Systematic Review," 2022.
- [14] R. Kaur and A. Doegar, "Brain tumor segmentation using deep learning: taxonomy, survey and challenges," in *Brain Tumor MRI Image Segmentation Using Deep Learning Techniques*, pp. 225–238, Elsevier, 2022.
- [15] M. Nazir, S. Shakil, and K. Khurshid, "Role of deep learning in brain tumor detection and classification (2015 to 2020): A review," *Computerized Medical Imaging and Graphics*, vol. 91, p. 101940, jul 2021.
- [16] A. Santhosh, T. Saranya, S. Sundar, and S. Natarajan, "Deep Learning Techniques for Brain Tumor Diagnosis: A Review," *Proceedings of the 4th International Conference on Microelectronics, Signals and Systems, ICMSS 2021*, 2021.
- [17] R. Yang, Y. Du, X. Weng, Z. Chen, S. Wang, and X. Liu, "Automatic recognition of bladder tumours using deep learning technology and its clinical application," *The International Journal of Medical Robotics and Computer Assisted Surgery*, vol. 17, apr 2021.
- [18] K. H. Cha, L. Hadjiiski, R. K. Samala, H.-P. Chan, E. M. Caoili, and R. H. Cohan, "Urinary bladder segmentation in CT urography using deep-learning convolutional neural network and level sets," *Medical Physics*, vol. 43, pp. 1882–1896, mar 2016.
- [19] I. Lorencin, N. Anđelić, J. Španjol, and Z. Car, "Using multi-layer perceptron with Laplacian edge detector for bladder cancer diagnosis," *Artificial Intelligence in Medicine*, vol. 102, p. 101746, jan 2020.
- [20] S. A. Harmon, T. H. Sanford, G. T. Brown, C. Yang, S. Mehralivand, J. M. Jacob, V. A. Valera, J. H. Shih, P. K. Agarwal, P. L. Choyke, and B. Turkbey, "Multiresolution Application of Artificial Intelligence in Digital Pathology for Prediction of Positive Lymph Nodes From Primary Tumors in Bladder Cancer," *JCO Clinical Cancer Informatics*, pp. 367–382, nov 2020.
- [21] X. Ma, L. M. Hadjiiski, J. Wei, H. Chan, K. H. Cha, R. H. Cohan, E. M. Caoili, R. Samala, C. Zhou, and Y. Lu, "U-Net based deep learning bladder segmentation in <scp>CT</scp> urography," *Medical Physics*, vol. 46, pp. 1752–1765, apr 2019.
- [22] N. Coudray, P. S. Ocampo, T. Sakellaropoulos, N. Narula, M. Snuderl, D. Fenyö, A. L. Moreira, N. Razavian, and A. Tsigos, "Classification and mutation prediction from non-small cell lung cancer histopathology images using deep learning," *Nature Medicine*, vol. 24, pp. 1559–1567, oct 2018.
- [23] A. Cruz-Roa, H. Gilmore, A. Basavanahally, M. Feldman, S. Ganesan, N. N. Shih, J. Tomaszewski, F. A. González, and A. Madabhushi, "Accurate and reproducible invasive breast cancer detection in whole-slide images: A Deep Learning approach for quantifying tumor extent," *Scientific Reports*, vol. 7, p. 46450, apr 2017.
- [24] Y. Bar, I. Diamant, L. Wolf, S. Lieberman, E. Konen, and H. Greenspan, "Chest pathology detection using deep learning with non-medical training," in *2015 IEEE 12th International Symposium on Biomedical Imaging (ISBI)*, vol. 2015-July, pp. 294–297, IEEE, apr 2015.
- [25] S. J. S. Gardezi, A. Elazab, B. Lei, and T. Wang, "Breast Cancer Detection and Diagnosis Using Mammographic Data: Systematic Review," *Journal of Medical Internet Research*, vol. 21, p. e14464, jul 2019.

- [26] S. Sharma and K. Guleria, "Deep Learning Models for Image Classification: Comparison and Applications," *2022 2nd International Conference on Advance Computing and Innovative Technologies in Engineering (ICACITE)*, pp. 1733–1738, apr 2022.
- [27] G. Yao, T. Lei, and J. Zhong, "A review of Convolutional-Neural-Network-based action recognition," *Pattern Recognition Letters*, vol. 118, pp. 14–22, feb 2019.
- [28] J. Naranjo-Torres, M. Mora, R. Hernández-García, R. J. Barrientos, C. Fredes, and A. Valenzuela, "A Review of Convolutional Neural Network Applied to Fruit Image Processing," *Applied Sciences*, vol. 10, p. 3443, may 2020.
- [29] S. Serte, A. Serener, and F. Al-Turjman, "Deep learning in medical imaging: A brief review," *Transactions on Emerging Telecommunications Technologies*, vol. 33, oct 2022.
- [30] A. Ajit, K. Acharya, and A. Samanta, "A Review of Convolutional Neural Networks," in *2020 International Conference on Emerging Trends in Information Technology and Engineering (ic-ETITE)*, pp. 1–5, IEEE, feb 2020.
- [31] H.-C. Shin, H. R. Roth, M. Gao, L. Lu, Z. Xu, I. Nogues, J. Yao, D. Mollura, and R. M. Summers, "Deep Convolutional Neural Networks for Computer-Aided Detection: CNN Architectures, Dataset Characteristics and Transfer Learning," *IEEE Transactions on Medical Imaging*, vol. 35, pp. 1285–1298, may 2016.
- [32] W. L. Alyoubi, W. M. Shalash, and M. F. Abulkhair, "Diabetic retinopathy detection through deep learning techniques: A review," *Informatics in Medicine Unlocked*, vol. 20, p. 100377, 2020.
- [33] Z. Wang, Q. Liang, F. Duarte, F. Zhang, L. Charron, L. Johnsen, B. Cai, and C. Ratti, "Quantifying legibility of indoor spaces using Deep Convolutional Neural Networks: Case studies in train stations," *Building and Environment*, vol. 160, p. 106099, aug 2019.
- [34] V. Sharma and R. N. Mir, "A comprehensive and systematic look up into deep learning based object detection techniques: A review," *Computer Science Review*, vol. 38, p. 100301, nov 2020.
- [35] M. M. Kasar, D. Bhattacharyya, and T.-h. Kim, "Face Recognition Using Neural Network: A Review," *International Journal of Security and Its Applications*, vol. 10, pp. 81–100, mar 2016.
- [36] X. Wu, D. Sahoo, and S. C. Hoi, "Recent advances in deep learning for object detection," *Neurocomputing*, vol. 396, pp. 39–64, jul 2020.
- [37] M. Mcuba, A. Singh, R. A. Ikuesan, and H. Venter, "The Effect of Deep Learning Methods on Deepfake Audio Detection for Digital Investigation," *Procedia Computer Science*, vol. 219, pp. 211–219, 2023.
- [38] M. M. Taye, "Theoretical Understanding of Convolutional Neural Network: Concepts, Architectures, Applications, Future Directions," *Computation*, vol. 11, p. 52, mar 2023.
- [39] S. Batra, S. S. Malhi, G. Singh, and M. Mahajan, "A brief overview on deep learning methods for lung cancer detection using medical imaging," *Think India Journal*, vol. 22, no. 30, pp. 1279–1288, 2019.